

ARTICLE

Received 14 Dec 2011 | Accepted 31 May 2012 | Published 3 Jul 2012

DOI: 10.1038/ncomms1938

Reprogramming of tRNA modifications controls the oxidative stress response by codon-biased translation of proteins

Clement T.Y. Chan^{1,2,†}, Yan Ling Joy Pang¹, Wenjun Deng¹, I. Ramesh Babu¹, Madhu Dyavaiah³, Thomas J. Begley³ & Peter C. Dedon^{1,4}

Selective translation of survival proteins is an important facet of the cellular stress response. We recently demonstrated that this translational control involves a stress-specific reprogramming of modified ribonucleosides in tRNA. Here we report the discovery of a step-wise translational control mechanism responsible for survival following oxidative stress. In yeast exposed to hydrogen peroxide, there is a Trm4 methyltransferase-dependent increase in the proportion of tRNA^{Leu(CAA)} containing m⁵C at the wobble position, which causes selective translation of mRNA from genes enriched in the TTG codon. Of these genes, oxidative stress increases protein expression from the TTG-enriched ribosomal protein gene *RPL22A*, but not its unenriched paralogue. Loss of either *TRM4* or *RPL22A* confers hypersensitivity to oxidative stress. Proteomic analysis reveals that oxidative stress causes a significant translational bias towards proteins coded by TTG-enriched genes. These results point to stress-induced reprogramming of tRNA modifications and consequential reprogramming of ribosomes in translational control of cell survival.

¹ Department of Biological Engineering, Massachusetts Institute of Technology, 77 Massachusetts Avenue, Cambridge, 02139, USA. ² Department of Chemistry, Massachusetts Institute of Technology, Cambridge, 02139, USA. ³ College of Nanoscale Science and Engineering, University at Albany, SUNY, Albany, New York 12203, USA. ⁴ Center for Environmental Health Sciences, Massachusetts Institute of Technology, Cambridge, 02139, USA. † Present address: Department of Biomedical Engineering, Boston University, 44 Cummington Street, MA 02215, USA. Correspondence and requests for materials should be addressed to P.C.D. (email: pcdedon@mit.edu).

Decades of study have revealed more than 100 ribonucleoside structures incorporated as post-transcriptional modifications mainly in transfer RNA and ribosomal RNA, with 25–35 modifications present in any one organism^{1–4}. In general, tRNA modifications enhance ribosome-binding affinity, reduce misreading and modulate frame shifting, all of which affect the rate and fidelity of translation^{5–8}. Emerging evidence points to a critical role for tRNA and rRNA modifications in the various cellular responses to stimuli, such as tRNA stability^{9,10}, transcription of stress response genes^{11–13} and control of cell growth¹⁴.

We recently used high-throughput screens and targeted analyses to show that the tRNA methyltransferase 9 (Trm9) modulates the toxicity of methylmethanesulfonate in *Saccharomyces cerevisiae*^{12,15}. This is similar to the observed role of Trm9 in modulating the toxicity of ionizing radiation¹⁶ and of Trm4 and other translation associated proteins in promoting viability after methylation damage^{15,17}. Trm9 catalyses the methyl esterification of the uracil-based cm⁵U and cm⁵s²U to mcm⁵U and mcm⁵s²U, respectively, at the wobble positions of tRNA^{UCU}-ARG and tRNA^{UUC}-GLU, among others¹⁸. These wobble base modifications enhance binding of the anticodon with specific codons in mixed codon boxes¹⁹. Codon-specific reporter assays and genome-wide searches revealed that Trm9-catalysed tRNA modifications enhanced the translation of AGA- and GAA-rich transcripts that functionally mapped to processes associated with protein synthesis, metabolism and stress signalling¹². These results lead to a model in which messenger RNA possessing specific codons will be more efficiently translated by tRNA, with anticodons containing the Trm9-modified ribonucleoside and that tRNA modifications can dynamically change in response to stress.

To study the functional dynamics of this conserved system, we recently developed a bioanalytical platform to quantify the spectrum of ribonucleoside modifications and we used it to assess the role of RNA modifications in the stress response of *S. cerevisiae*²⁰. This approach led to the discovery of signature changes in the spectrum of tRNA modifications in the cellular response to mechanistically different toxicants. Exposure of yeast to hydrogen peroxide (H₂O₂), as a model oxidative stressor, led to increases in the levels of 2'-O-methylcytosine (Cm), 5-methylcytosine (m⁵C) and N²,N²-dimethylguanosine (m²2G), whereas these ribonucleosides decreased or were unaffected by exposure to methylmethanesulfonate, arsenite and hypochlorite²⁰. Loss of the methyltransferase enzymes catalysing the formation of the modified ribonucleosides led to cytotoxic hypersensitivity to H₂O₂ exposure²⁰. These results support a general model of dynamic control of tRNA modifications in cellular response pathways and expand the repertoire of mechanisms controlling translational responses in cells.

In the present study, we have used a variety of bioanalytical and bioinformatic approaches to define a step-wise mechanistic link between tRNA modifications and the oxidative stress response. Following an oxidative stress, reprogramming of a specific tRNA wobble modification leads to selective translation of mRNA species enriched with the cognate codon. Among the codon-biased, selectively translated proteins is one member of a pair of ribosomal protein paralogues, and the loss of this paralogue causes sensitivity to oxidative stress. These results lead to a model in which stress-induced reprogramming of tRNA modifications and the associated reprogramming of ribosomes provides translational control of cell survival following an oxidative stress.

Results

H₂O₂ increases m⁵C at the wobble position of tRNA^{Leu(CAA)}. In *S. cerevisiae*, m⁵C is synthesized by Trm4 methyltransferase (also called Ncl1) and we previously observed that the level of m⁵C in total tRNA increased following exposure to H₂O₂ (ref. 20), with loss of Trm4 causing hypersensitivity to the cytotoxic effects of H₂O₂ (ref. 20). To rule out second site mutations as the cause of

this phenotype, we performed a complementation study using a *TRM4* expression vector in the *trm4* mutant strain and observed that re-expression of Trm4 conferred resistance to H₂O₂ exposure (Supplementary Fig. S1 and Supplementary Methods).

Although m⁵C is present in at least 34 species of tRNA², tRNA^{Leu(CAA)} is the only tRNA with m⁵C at the anticodon wobble position 34, as well as position 48 at the junction between the variable and TΨC loops². To determine whether H₂O₂ exposure altered the levels of m⁵C at one or both of these positions, tRNA^{Leu(CAA)} was purified from H₂O₂-exposed and unexposed cells by sequential gel and affinity purification. The resulting purified tRNA^{Leu(CAA)} was digested with RNase T1 to give a signature 4-mer oligonucleotide harbouring either C or m⁵C at position 48 (CAAG) (Fig. 1a). In addition, total tRNA from H₂O₂-exposed and unexposed *S. cerevisiae* was digested with RNase U2 to produce another unique 5-mer oligonucleotide with C or m⁵C at position 34 of tRNA^{Leu(CAA)} (UUCAA) (Fig. 1a). As shown in Fig. 1b, subsequent mass spectrometric analysis of these oligonucleotides revealed that H₂O₂ exposure caused a 70% increase in m⁵C at the wobble position and a 20% decrease at position 48.

m⁵C controls the translation of UUG-enriched mRNA. Next, we asked if the presence of m⁵C in tRNA^{Leu(CAA)} enhanced the translation of UUG-containing mRNA, given the evidence that m⁵C at the wobble position of the leucine-inserting amber suppressor tRNA^{Leu(CUA)} enhances translation²¹. To test this hypothesis, we used a dual Renilla and Firefly luciferase reporter construct²² (illustrated in Fig. 2a), in which the linker region connecting these two in-frame coding sequences was either four random or four TTG codons in a row (control and 4X-TTG, respectively). Expression of the Firefly luciferase portion of the reporter fusion protein is thus dependent upon the efficiency of translating the linker region²². The expression of both the Renilla and Firefly luciferase reporters was quantified under conditions of oxidative stress and loss of Trm4 activity (Fig. 2b, Supplementary Fig. S2). As shown in Fig. 2b, loss of Trm4 caused a 9.6-fold reduction in 4X-TTG reporter expression relative to wild-type cells under basal conditions. Following H₂O₂ treatment, there was an even larger 23.8-fold reduction in 4X-TTG reporter activity in *trm4Δ* cells compared with wild-type cells, with 4X-TTG reporter expression in wild-type cells unaffected by H₂O₂ exposure (Fig. 2b). Effects of this magnitude were not observed for the control reporter, which was devoid of TTG codons in the linker region (Supplementary Fig. S2). The *trm4Δ* cells containing the control reporter had an H₂O₂-induced twofold decrease in Firefly luciferase expression, relative to untreated cells, suggesting contributions by Trm4 to some aspect of general translation during oxidative stress. Taken together, these results are consistent with the idea that translation of TTG-rich sequences is facilitated by Trm4-catalysed tRNA modifications and that m⁵C modifications have an important role in the translational response to H₂O₂ exposure. Coupled with the evidence for H₂O₂-induced increases in m⁵C at the wobble position of tRNA^{Leu(CAA)}, the data support a model in which oxidative stress causes a Trm4-mediated increase in the incorporation of m⁵C in tRNA^{Leu(CAA)}, with the methylated wobble base enhancing the translation of mRNA from genes enriched in TTG codon usage for leucine.

Differential codon enrichment in genes for ribosomal protein paralogues. This direct link between a tRNA wobble modification, codon usage and gene expression immediately raised the question of biases in the distribution of the TTG codon in genes that have a role in responding to oxidative stress. Using a recently developed *S. cerevisiae* codon distribution database²³, we quantified TTG codon use across the yeast genome. An average of 29% of leucines are coded by TTG in the 5,782 genes analysed. However, in 38 genes, more than 90% of the leucines are coded by TTG. Intriguingly,

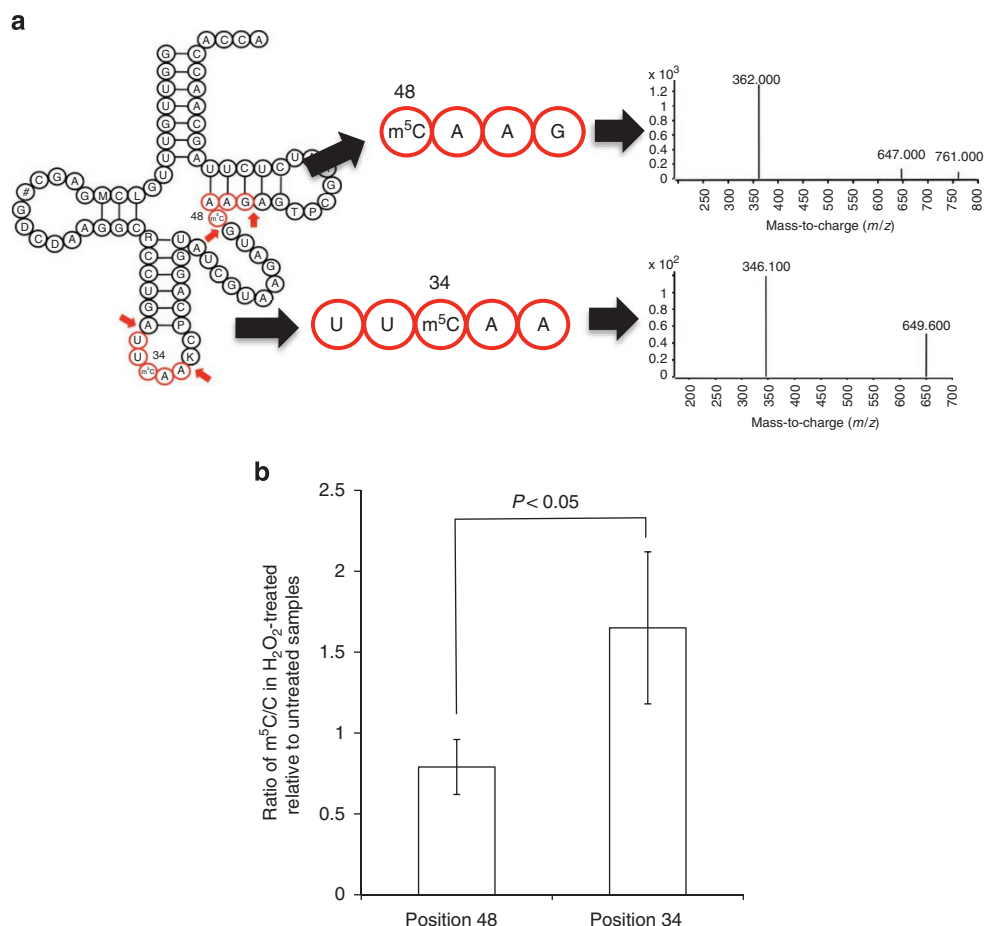


Figure 1 | H₂O₂ exposure increases the level of m⁵C at the wobble position of tRNA^{Leu(CAA)}. (a) tRNA^{Leu(CAA)} was digested with ribonucleases to generate oligoribonucleotides containing m⁵C or C at position 34 (CAAG) or position 48 (UUCAA), and the oligoribonucleotides were quantified by mass spectrometry. (b) The graph shows the ratio of m⁵C/C in tRNA^{Leu(CAA)} from H₂O₂-treated cells relative to untreated cells. The data represent mean \pm s.d. for three experiments. The data for position 34 are significantly different from those for position 48 by Student's *t*-test with $P < 0.05$.

among these 38 genes, 26 encoded ribosomal proteins and the others are loosely related to energy metabolism (Table 1). These 26 ribosomal proteins represent a subset of the 138 such proteins encoded by the yeast genome. Of the 78 proteins that comprise a ribosome in *S. cerevisiae*, 59 occur in homologous pairs, or paralogues, that are believed to have arisen by an evolutionary genome duplication event²⁴. Recent evidence supports a model in which individual paralogues have different functional roles in a variety of cell processes in yeast^{25–28}, with studies by Komili *et al.*²⁹ revealing that a specific set of ribosomal protein homologues is necessary for the translation of ASH1 mRNA during bud tip formation. One striking feature of the genes encoding paralogous ribosomal proteins is a bias in frequency of TTG codon use, as shown in Supplementary Tables S1 and S2. For example, 100% and 34% of the leucines in the paralogues Rpl22A and Rpl22B, respectively, are coded by TTG.

H₂O₂ increases a TTG-enriched ribosomal protein paralogue. The biased distribution of TTG codons in ribosomal protein paralogues raised another question: will H₂O₂-induced increases in m⁵C in tRNA^{Leu(CAA)} lead to selective expression of TTG-enriched ribosomal protein paralogues? To test this hypothesis, we used a mass spectrometry-based proteomics approach to determine the relative quantities of several ribosomal protein paralogues in wild-type and *trm4Δ* mutant yeasts exposed to H₂O₂. The study entailed isolation of polysomes from lysates of H₂O₂-treated and control yeast cells by differential ultracentrifugation, followed by trypsin digestion of the

proteins and quantification of the tryptic peptides by liquid chromatography-coupled high-resolution mass spectrometry (LC-MS). Using this approach, we were able to consistently identify 39 ribosomal proteins in each of three biological replicates (Supplementary Table S3), including seven pairs of distinguishable paralogues (Rpl6a/b, Rpl7a/b, Rpl16a/b, Rpl22a/b, Rpl33a/b, Rpl36a/b and Rps7a/b) (Supplementary Tables S3 and S4). Although the amino acid sequences of each set of paralogous proteins are nearly identical, they contain at least one signature tryptic peptide that could be used to identify and quantify each of 14 ribosomal paralogues in the mixture (Supplementary Table S4). A protein BLAST search in the NCBI database using these peptide sequences confirmed that the peptides were unique to the specific *S. cerevisiae* ribosomal proteins (data not shown). Further, the sequence identity of these unique peptides was confirmed by the analysis of the b- and y-ion series in collision-induced dissociation (CID) spectra (Supplementary Fig. S3).

This approach was applied to determine the relative quantities of ribosomal homologues Rpl22a and Rpl22b, in which 100% and 34% of the leucines were coded by TTG, respectively. In the absence of absolute quantification of individual proteins, changes in the protein levels are expressed as changes in the ratio of the signals for the signature peptides from the protein pairs (for example, Rpl22a/Rpl22b). The LC-MS signal ratios for the 14 ribosomal paralogues are shown in Supplementary Tables S5 and S6. A comparison of wild-type and *trm4Δ* mutants revealed that loss of *TRM4*

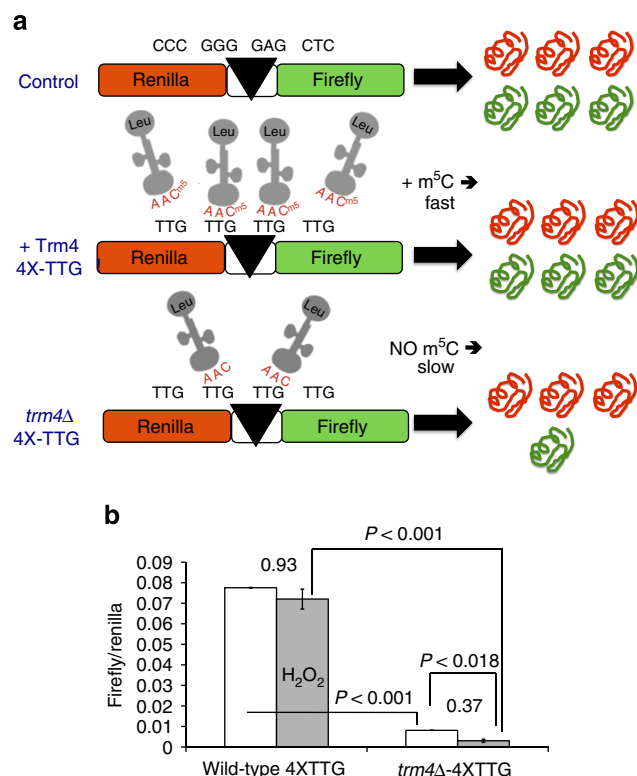


Figure 2 | H₂O₂ and Trm4 methyltransferase control gene expression at the level of TTG codon usage. (a) Scheme illustrating the dual luciferase reporter system for assessing the effect of TTG codon usage on protein expression in wild-type and *trm4Δ* mutant yeast cells transformed with either control or 4X-TTG reporter plasmids. (b) Control and 4X-TTG reporter activity was quantified in H₂O₂-exposed (grey bars) and unexposed (white bars) wild-type or *trm4Δ* cells. The ratio of treated to untreated is indicated above each condition. Data represent mean \pm s.d. for three biological replicates.

caused a significant decrease in the ratio of Rpl22a to Rpl22b and of Rpl16b to Rpl16a (Fig. 3), the two sets of paralogues with the largest differences in TTG codon use (Supplementary Table S4). When wild-type and *trm4* cells were exposed to H₂O₂, the ratio of Rpl22a to Rpl22b increased significantly in the wild-type cells but not in the *trm4* mutants (Fig. 4). To determine whether these changes are indeed occurring at the level of translation, we quantified mRNA for both Rpl22a and Rpl22b by real-time quantitative PCR and we observed that the transcript levels remained unchanged following loss of *TRM4* or exposure to H₂O₂ (Supplementary Table S7).

H₂O₂ enhances translation of proteins with TTG-enriched genes.

Having performed a targeted analysis of ribosomal proteins that revealed evidence of selective translation of TTG-enriched proteins, we next undertook a more general proteomic analysis of H₂O₂-induced differences in the ~200 most abundant proteins in yeast (Supplementary Data 1), using a SILAC-based approach to quantify changes in the abundance of proteins in H₂O₂-induced cells³⁰. As shown in Fig. 5, proteins with high TTG usage are more likely to be downregulated (Fig. 5a, $P=0.048$ by Student's *t*-test) as a consequence of loss of Trm4 activity, whereas these proteins are significantly upregulated in wild-type cells exposed to H₂O₂ (Fig. 5b, $P=6.41 \times 10^{-7}$). However, oxidative stress did not affect the expression of proteins from TTG-enriched genes in *trm4Δ* cells (Fig. 5c, $P=0.554$), which is consistent with a role for m⁵C in the selective translation of UUG-enriched mRNA species.

Analysis of the functional categories of proteins affected by H₂O₂ exposure (Supplementary Fig. S4) reveals that proteins related to translation are significantly upregulated by oxidative stress, which is consistent with the analysis of ribosomal protein expression in Fig. 4, although Rpl22A and Rpl22B could not be differentiated likely as a result of the minimal sequence difference between the two proteins. One interesting complication apparent in Fig. 5b is that proteins from genes with intermediate TTG frequencies (that is, frequencies between the unchanged and upregulated fractions) are significantly downregulated in both H₂O₂-exposed wild-type cells ($P=0.022$) and *trm4Δ* mutants ($P=0.048$). This illustrates the limitations of our model for selective expression of TTG-enriched genes following oxidative stress and suggests that other layers of translational control are operant in the response to H₂O₂ exposure.

Rpl22A is required for the oxidative stress response in yeast.

To further refine the mechanistic link between H₂O₂ exposure, m⁵C modification of tRNA and Rpl22A expression as a survival response, we assessed the H₂O₂ sensitivity of yeast strains lacking individual Rpl16A/B and Rpl22A/B paralogues. As shown in Fig. 6, only the loss of *RPL22A* conferred sensitivity to H₂O₂, whereas the loss of *RPL16A*, *RPL16B* and *RPL22B* did not affect H₂O₂-induced cytotoxicity. The magnitude of the increased cytotoxicity caused by loss of Rpl22A (20 to 10% survival) is similar to the change in cytotoxicity that we observed previously for loss of Trm4 (ref. 20). This suggests that Rpl22A contributes significantly to the oxidative stress survival response in yeast. The lack of effect of Rpl16b loss on H₂O₂ toxicity, in spite of the Trm4-dependence of this TTG-enriched paralogue (Fig. 3), suggests that it shares functional equivalence with Rpl16a in ribosomes.

Discussion

Using a combination of bioanalytical and bioinformatic tools, we have defined a step-wise translational control mechanism responsible for cell survival following oxidative stress, a model for which is shown in Fig. 7. Although some of the individual steps in this model could be explained by other phenomena, such as tRNA or protein stability, there are few, if any, alternative mechanisms that could explain the sum of the observed behaviours. The first step in this model involves H₂O₂-induced increases in the level of m⁵C at the wobble position of tRNA^{Leu(CAA)} (Fig. 7a) with a concomitant decrease in m⁵C at the neighbouring position 48 in the same tRNA. The observation of a 70% increase in the proportion of tRNA^{Leu(CAA)} molecules containing a wobble m⁵C is consistent with a simple increase in TRM4 activity acting on a fixed concentration of total tRNA^{Leu(CAA)}. Alternatively, the proportion of m⁵C-containing tRNA^{Leu(CAA)} could remain constant, with an increase in transcription leading to an increase in the total number of copies of tRNA^{Leu(CAA)}, or both transcription and TRM4 activity could increase to raise the concentration of tRNA^{Leu(CAA)} with m⁵C. Finally, given the precedent for stress-induced degradation of tRNA^{9,10}, oxidative stress could lead to selective degradation of unmethylated tRNA^{Leu(CAA)}. By any mechanism, the data show that oxidative stress increases the proportion of tRNA^{Leu(CAA)} containing m⁵C at the wobble position, with an absolute requirement for Trm4 activity for the existence of m⁵C (ref. 20).

The second step in the model posits that the increase in m⁵C in tRNA^{Leu(CAA)} enhances the efficiency of translation of mRNAs enriched in the UUG codon recognized by this tRNA (Fig. 7b). This is supported by the reporter assay results shown in Fig. 2, with loss of Trm4 activity having no or little effect on reporter expression when TTG usage is low but causing a sharp decrease in expression when TTG usage is high. This is consistent with the observation that loss of Trm4, and thus m⁵C, decreases the expression of TTG-enriched proteins but not unenriched proteins (Figs 3 and 5). The observation using the unmodified reporter (Supplementary Fig. S2)

Table 1 | *S. cerevisiae* genes with $\geq 90\%$ TTG codon usage for leucine.

Gene name	No. of TTG	Freq. of TTG*	Protein function
<i>RPL15A</i>	13	1	Protein component of the large (60S) ribosomal subunit
<i>RPL28</i>	9	1	Ribosomal protein of the large (60S) ribosomal subunit
<i>RPL39</i>	2	1	Protein component of the large (60S) ribosomal subunit
<i>RPS10B</i>	9	1	Protein component of the small (40S) ribosomal subunit
<i>CCW12</i>	9	1	Cell wall mannoprotein
<i>RPL22A</i>	7	1	Protein component of the large (60S) ribosomal subunit
<i>RPL43A</i>	3	1	Protein component of the large (60S) ribosomal subunit
<i>RPL37B</i>	2	1	Protein component of the large (60S) ribosomal subunit
<i>RPL37A</i>	2	1	Protein component of the large (60S) ribosomal subunit
<i>HYP2</i>	11	1	Translation elongation factor eIF-5A
<i>RPS15</i>	9	1	Protein component of the small (40S) ribosomal subunit
<i>RPL36B</i>	6	1	Protein component of the large (60S) ribosomal subunit
<i>NOP10</i>	5	1	Constituent of small nucleolar ribonucleoprotein particles
<i>RPS26B</i>	4	1	Protein component of the small (40S) ribosomal subunit
<i>HSP12</i>	3	1	Plasma membrane localized protein
<i>TDH3</i>	20	0.95	Glyceraldehyde-3-phosphate dehydrogenase, isozyme 3
<i>TDH2</i>	20	0.95	Glyceraldehyde-3-phosphate dehydrogenase, isozyme 2
<i>TDH1</i>	19	0.95	Glyceraldehyde-3-phosphate dehydrogenase, isozyme 1
<i>RPL8A</i>	19	0.95	Ribosomal protein L4 of the large (60S) ribosomal subunit
<i>RPS6B</i>	19	0.95	Protein component of the small (40S) ribosomal subunit
<i>RPS6A</i>	19	0.95	Protein component of the small (40S) ribosomal subunit
<i>RPL10</i>	16	0.94	Protein component of the large (60S) ribosomal subunit
<i>RPL4A</i>	26	0.93	Protein component of the large (60S) ribosomal subunit
<i>RPL4B</i>	26	0.93	Protein component of the large (60S) ribosomal subunit
<i>RPS13</i>	13	0.93	Protein component of the small (40S) ribosomal subunit
<i>RPS5</i>	13	0.93	Protein component of the small (40S) ribosomal subunit
<i>ENO2</i>	35	0.92	Enolase II
<i>ANB1</i>	11	0.92	Translation elongation factor eIF-5A
<i>CDC19</i>	32	0.91	Pyruvate kinase
<i>RPL12B</i>	10	0.91	Protein component of the large (60S) ribosomal subunit
<i>PDC1</i>	49	0.91	Major of three pyruvate decarboxylase isozymes
<i>RPS2</i>	19	0.90	Protein component of the small (40S) subunit
<i>RPL8B</i>	19	0.90	Ribosomal protein L4 of the large (60S) ribosomal subunit
<i>ENO1</i>	36	0.90	Enolase I
<i>RPL17A</i>	9	0.90	Protein component of the large (60S) ribosomal subunit
<i>RPL17B</i>	9	0.90	Protein component of the large (60S) ribosomal subunit
<i>RPS9B</i>	18	0.90	Protein component of the small (40S) ribosomal subunit
<i>RPL9A</i>	9	0.90	Protein component of the large (60S) ribosomal subunit

*Proportion of leucines encoded by TTG.

that H₂O₂ exposure of wild-type cells did not affect reporter expression levels, yet it decreased reporter expression in the *trm4Δ* mutant, points to contributions by factors other than modification-specific codon usage in the control of translation during the oxidative stress response.

In addition to the proteome changes shown in Fig. 5, the observed changes in expression of ribosomal proteins Rpl22A and Rpl16B (Figs 3 and 4) are consistent with the idea that oxidative stress enhances the translation of UUG-biased mRNAs. The pair of ribosomal gene paralogues with the widest difference in the use of TTG for coding leucine, *RPL22A* at 100% and *RPL22B* at 38%, showed the largest changes in protein expression following H₂O₂ exposure, with expression of the high TTG usage *RPL22A* increasing with oxidative stress and decreasing with loss of *TRM4* (Fig. 4). The latter result points to the translational control of Rpl22A by Trm4, with the absolute requirement of oxidation-induced increases in m⁵C for the enhanced expression of Rpl22A. Although we cannot rule out differential protein stability as a determinant of the proportions of the ribosomal protein paralogues, differences in leucine content do not account for the differential stability of Rpl22A and Rpl22B. The paralogues differ minimally in leucine content and the changes in paralogue levels caused by loss of *TRM4* do not correlate with this amino acid. Although Rpl22A and Rpl22B have 7 and 8 leucines, respectively, and the relative amount of Rpl22A decreases with loss

of *TRM4*, Rpl16A and Rpl16B have 17 and 18 leucines, respectively, yet the relative quantity of Rpl16A decreases with loss of *TRM4*. Further, the data presented here do not provide insights into the function of ribosomes with TTG-enriched ribosomal proteins, such as their potential role in selective translation of mRNAs enriched with TTG or other codons, or their possible role in the early and late stages of the oxidative stress response. A detailed analysis of ribosome-bound mRNAs or nascent peptides in the early and late stages of the oxidative stress response would shed light on these issues. When considered with the other results, our observations suggest that the H₂O₂-induced increase in the level of the Rpl22a ribosomal protein is caused, at least in part, by Trm4-mediated changes in m⁵C levels in tRNA with subsequent control of translation of mRNA arising from TTG-enriched genes.

The mechanistic connection between Trm4 and Rpl22A is further established by the observation that loss of either protein makes corresponding *trm4Δ*²⁰ or *rpl22aΔ* (Fig. 6) cells sensitive to H₂O₂. There are parallels for the H₂O₂-sensitive phenotype of *rpl22aΔ* in the recently defined roles of other ribosomal proteins in the oxidative stress response in higher eukaryotes. One example also serves as an illustration of the ribosome filter hypothesis concerning selective translation of mRNA³¹: human ribosomal protein Rpl26 regulates translation of p53, a major node in oxidative stress response³², by interacting with the 5'-untranslated region of p53 mRNA³³.

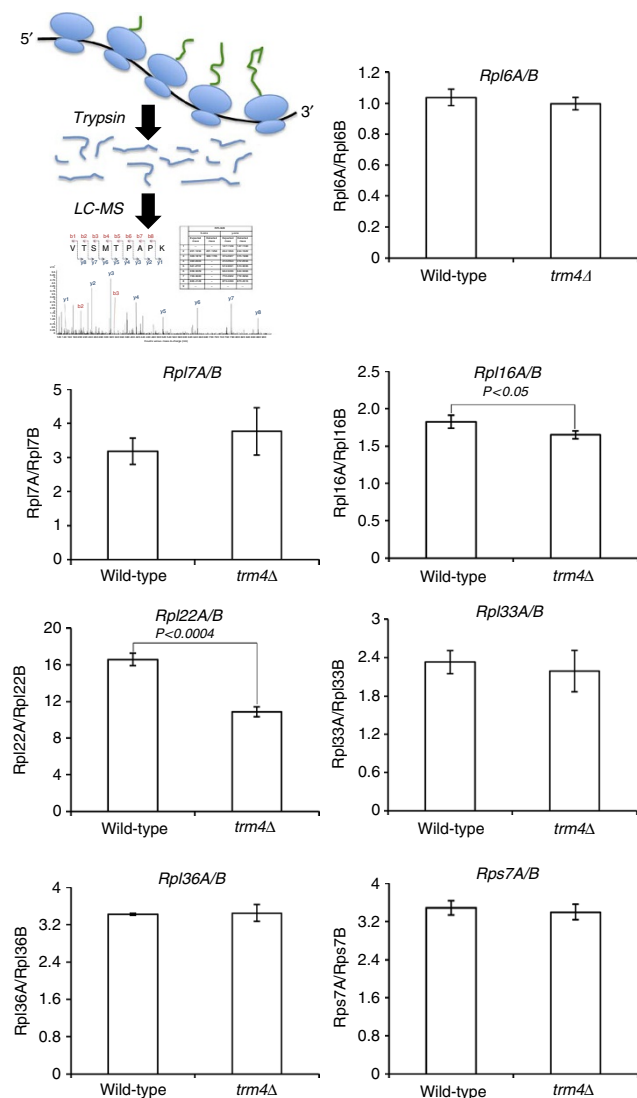


Figure 3 | Loss of Trm4 methyltransferase decreases the proportion of ribosomes containing TTG codon-enriched ribosomal protein paralogs. Ribosomal proteins in wild-type and *trm4Δ* mutant *S. cerevisiae* were quantified by LC-MS/MS (schematic inset) and the relative quantities of ribosomal protein paralogs presented as the ratio of the signal intensity for the paralogue with high TTG usage to that of the low-usage paralogue. Data represent mean \pm s.d. for three biological replicates. *P* values denote statistically significant differences by Student's *t*-test.

Similarly, the highly conserved Rpl22 (ref. 34) is involved in the activation of internal ribosomal entry site-mediated translation in response to several types of stress^{35,36} and it participates in murine T-cell development by regulating translation of p53 (ref. 37). Interestingly, ribosomal proteins may have roles in stress response other than ribosome structure, as suggested by recent observations of Rpl22 involvement in non-ribosomal ribonucleoprotein complexes such as the telomerase holoenzyme^{36,38–40}.

This series of observations leads to a model (Fig. 7) in which oxidative stress causes an early increase in Trm4-mediated m⁵C levels in tRNA^{Leu(CAA)}, which leads to selective translation of UUG-enriched mRNAs, including ribosomal protein paralogue Rpl22a and other proteins derived from many TTG-enriched genes. Clearly, this model does not address the complexity of translational control mechanisms, as suggested by the proteomic analysis shown in Fig. 5, in which mRNA from genes with varying enrichment of

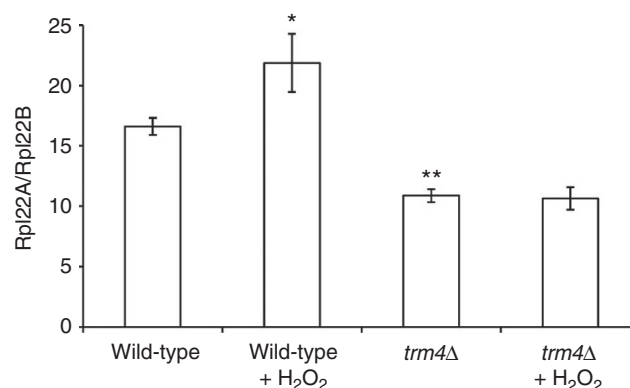


Figure 4 | H₂O₂ exposure increases the proportion of ribosomes containing ribosomal protein paralogue Rpl22a in wild-type *S. cerevisiae* but not in *trm4Δ* mutants. Cells were exposed to 2 mM H₂O₂ for 1 h and the quantities of ribosomal proteins were determined by LC-MS/MS analysis. Data are expressed as the ratio of the TTG-enriched paralogue Rpl22a to unenriched Rpl22b. Data represent mean \pm s.d. of three biological replicates. Asterisks denote statistically significant differences between H₂O₂-treated and untreated cells as judged by Student's *t*-test with *P* < 0.05.

TTG codons are not necessarily subject to enhanced translational efficiency. This complexity is further illustrated by the possibility of reprogramming of other modifications, such as H₂O₂-induced increases in Cm and m²G (ref. 20), in other tRNA species, with subsequent selective expression of mRNAs enriched with other codons, as well as the potential for reprogramming of ribonucleoside modifications in rRNA species. Nonetheless, the present observations add to the growing recognition of a role for functional diversity in ribosome composition⁴¹ and a role for ribosomes in selective translation of proteins³¹. This reconfiguration of the translation machinery is similar to the proposed generation of 'immunoribosomes' as a subset of T-cell ribosomes responsible for translating peptides involved in antigen presentation⁴². The abundance of ribosomal protein paralogs, the variety of RNA modifications in tRNA and rRNA, and the established biases in codon distributions in genes suggest a mechanism capable of fine tuning the translational response to virtually any cell stimulus.

Methods

Codon reporter assay. The effect of TTG codon frequency on protein expression in wild-type and *trm4Δ* yeast cells was assessed using a dual luciferase reporter system²² in which Renilla luciferase is connected in-frame to Firefly luciferase by a 12-bp sequence (control: 5'-CCCGGGGAGCTC-3' or 4X-TTG: 5'-TTGTTGTGTTG-3'), all under the control of an *ADHI* promoter and *CYC1* terminator²². Following transformation with either control or 4X-TTG plasmid, cells were grown to $\sim 5 \times 10^6$ cells per ml and then treated with 2 mM H₂O₂ or H₂O for 60 min. Cell pellets were lysed by bead-beating in lysis buffer and lysates clarified by centrifugation. Luminescence reactions were initiated with Promega DLR (50 μ l; Promega; Madison, WI) added to clarified lysates (5 μ l) and measured using a Victor Plate Reader (PerkinElmer; Waltham, MA).

RNAse digestion of tRNA. Purified tRNA^{Leu(CAA)} (~ 2.5 μ g) was digested with RNase T1 (1 U; Ambion, Austin, TX) in 10 mM Tris buffer (pH 7.4, 37 $^{\circ}$ C, 1 h). RNase U2 (Thermo Scientific, Waltham, MA) digestion (4 U) was carried out using total tRNA (0.5 mg, 37 $^{\circ}$ C, 4 h). Oligoribonucleotides were dephosphorylated with alkaline phosphatase (10 U).

Quantifying m⁵C in tRNA^{Leu(CAA)}. RNase T1 and U2 digestion maps of tRNA were obtained using the Mongo Oligo Mass Calculator (v2.06; <http://library.med.utah.edu/masspec/mongo.htm>). Digested tRNA oligos were resolved by HPLC (C18 Hypersil GOLD aQ, 150 \times 2.1 mm, 3 μ m particle; Thermo Scientific) coupled to a triple quadrupole mass spectrometer (MS; 6410; Agilent Technologies, Santa Clara, CA) with an electrospray ionization source operated in negative ion mode. HPLC was performed with a gradient of acetonitrile in 8 mM ammonium acetate

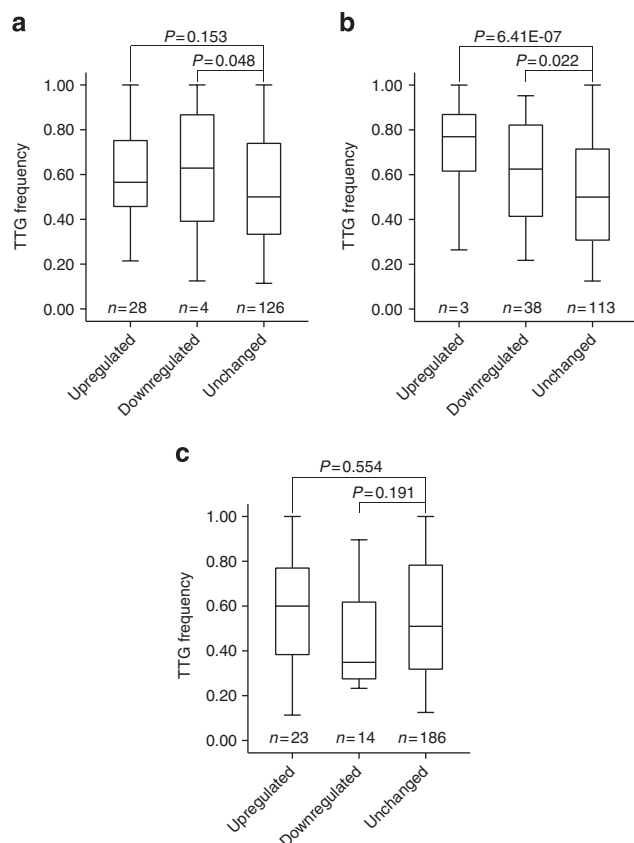


Figure 5 | SILAC-based proteomic analysis reveals that H_2O_2 enhances the translation of TTG-enriched proteins. Protein extracts from control and H_2O_2 -treated wild-type and *trm4* mutant yeast were mixed 1:1 with proteins from U- $[^{13}C,^{15}N]$ -lysine-labeled *lys1Δ* yeast cells as an internal standard³⁰. Protein mixtures were then subjected to trypsin digestion and proteomic analysis by LC-QTOF analysis. The quantities of the 261 most abundant proteins appearing in each of four biological replicates were analysed by Student's *t*-test ($P < 0.05$) for increased (upregulation), decreased (downregulation) or unchanged levels in **(a)** *trm4Δ* mutant versus wild-type cells, **(b)** H_2O_2 -treated versus untreated wild-type cells, and **(c)** H_2O_2 -treated versus untreated *trm4Δ* mutant cells. Within these three groups of proteins, the frequency of using TTG to code for leucine was calculated. The resulting frequency data are presented as a box-and-whiskers plot with the bar representing the median value, the box encompassing the range of data between the first and third quartile, and the error bars embracing data within 1.5-times interquartile range. Differences between upregulated, downregulated and unchanged categories were subjected to Student's *t*-test with the indicated *P* values.

(0.2 ml min⁻¹, 45 °C): 0–2 min, 1%; 2–30 min, 1–15%; 30–31 min, 15–100%; 31–41 min, 100%. MS parameters: drying gas, 325 °C and 81 ml min⁻¹; nebulizer, 30 p.s.i.; capillary voltage, 3,800 V; dwell time, 200 ms. The first and third MS quadrupoles were set to unit resolution and the oligos containing m⁵C were identified by comparison with standards and CID fragmentation patterns generated in a quadrupole time-of-flight MS. A selected ion chromatogram for a particular charge state of each oligo (unexposed and exposed to H_2O_2) was obtained, and the summation of the mass spectra over a particular peak was used for relative quantification of changes in m⁵C levels at positions 34 and 48 of tRNA^{Leu(CAA)}.

Ribosome isolation. Cells (10¹⁰) were resuspended in lysis buffer (10 ml) with 50 mM Tris-acetate, 50 mM ammonium chloride, 12 mM MgCl₂ and 1 mM dithiothreitol (pH 7) and lysed mechanically by bead-beating. Cell lysate was centrifuged (10,000g, 10 min), the supernatant collected, and centrifugation repeated twice to remove all particulates. The debris-free supernatant was layered over 2.5 ml of 1 M sucrose, 20 mM HEPES, 500 mM KCl, 2.5 mM magnesium acetate and 2 mM dithiothreitol at pH 7.4 and centrifuged for 110 min at 370,000g (*r*_{max}).

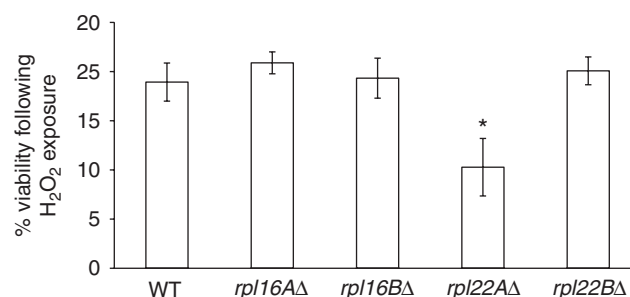


Figure 6 | Ribosomal protein paralogue Rpl22a confers resistance to H_2O_2 exposure in *S. cerevisiae*. Wild-type (WT) *S. cerevisiae* and strains lacking *RPL16A*, *RPL16B*, *RPL22A* or *RPL22B* were exposed to 5 mM H_2O_2 and survival was assayed as described in Methods. Data represent mean \pm s.d. of three biological replicates. The asterisk denotes a statistically significant difference compared with all other values in the figure, as judged by Student's *t*-test with $P < 0.05$.

Supernatant was removed and the pelleted ribosomes were resuspended in 1.5 ml of a digestion buffer with 100 mM ammonium acetate, pH 8.5. The samples were concentrated by spin dialysis on YM-10 filters. The concentrate was re-diluted with the digestion buffer and subject to spin dialysis five times to remove salts. Yield: ~300 μ g of protein.

Identification of ribosomal proteins. As the sequences of ribosomal protein paralogs are similar, we identified a unique tryptic peptide to quantify each paralogue. Following reduction with dithiothreitol (1 mM, 2 h, 37 °C) and alkylation with iodoacetamide (5.5 mM, 30 min, ambient temperature), purified ribosomal proteins (50 μ g) were digested with proteomics-grade trypsin (1 μ g) in 200 μ l of ammonium acetate solution (100 mM, pH 8.5, 37 °C, 12 h). Samples were lyophilized and resuspended in 100 μ l of 0.1% formic acid. Peptides in a portion of the tryptic digest (2.5 μ g, 5 μ l) were analysed by LC-MS on an Agilent 1200 capillary HPLC coupled to an Agilent 6520 QTOF MS (Agilent Technologies). Peptides were resolved on an Agilent ZORBAX 300SB-C18 column (100 \times 0.3 mm, 3 μ m particle) eluted with a gradient of acetonitrile in 0.1% formic acid (20 μ l min⁻¹, 45 °C): 0–25 min, 1–30%; 25–30 min, 30–60%; 30–31 min, 60–95%; 31–36 min, 95%. The MS was operated in positive ion mode with electrospray parameters as follows: fragmentor voltage, 110 V; drying gas, 300 °C and 51 ml min⁻¹; nebulizer, 20 p.s.i.; capillary voltage, 3,500 V. Peptide ions were scanned over $m/z = 100$ –1,700 at an acquisition rate of 1.4 spectra s⁻¹. Data analysis was performed with Agilent Mass Hunter Software and compounds were detected using molecular feature extractor with 300 count minimum peak height and maximum charge state of 2. The molecular feature extractor compound lists were subjected to peptide mass fingerprint analysis with the Agilent Spectrum Mill proteomics software to identify proteins based on peptide accurate mass. A search was performed against the NCBI protein sequence database for *S. cerevisiae* with no protein modifications and missed cleavage considered, and with a 20 p.p.m. mass tolerance and > 25% protein coverage.

Identified peptides were sequenced by LC-coupled quadrupole time-of-flight (QTOF) mass spectrometry using HPLC conditions described earlier and operating the QTOF in targeted tandem mass spectrometry (MS/MS) mode with acquisition rates for both MS and MS/MS scans at 1.4 spectra s⁻¹ and a constant collision energy of 15 V to selectively monitor ions of the peptides shown in Supplementary Table S4; other MS parameters were described earlier. Peptide CID spectra were acquired by targeted MS/MS analysis and the b- and y-ion assignments (Supplementary Fig. S3) used to determine the amino-acid sequence. A search of the NCBI protein sequence database confirmed that each peptide uniquely identified its corresponding ribosomal protein paralogue.

Relative quantification of ribosomal protein paralogs. With unique tryptic peptides for each paralogue (Supplementary Table S4), the selected ion chromatogram of each peptide at charge state +2 was extracted from the total ion chromatogram, with the MS signal intensity determined by summation of the area under the mass spectrum (Supplementary Tables S5 and S6). Signal intensities for the ribosomal protein paralogs were normalized by taking their ratio, with the high TTG paralogue in the numerator and low TTG in the denominator (Supplementary Tables S5 and S6). This ratio was then used to determine changes in the quantities of ribosomal protein paralogs in H_2O_2 -exposed cells (Figs 3 and 4).

SILAC proteomics. *Lys1Δ* yeast cells were grown in yeast nitrogen base medium containing 30 mg l⁻¹ of L-lysine-U- $[^{13}C]_6$, $[^{15}N]_2$ (Isotec-SIGMA, Miamisburg, OH) for ≥ 10 generations, until they reached log-phase (OD₆₀₀ ~ 0.7)⁴³. Wild-type and *trm4Δ* yeast cells were grown in yeast nitrogen base medium containing 30 mg l⁻¹ of L-lysine and were treated with 5 mM H_2O_2 at log-phase²⁰. Cells were

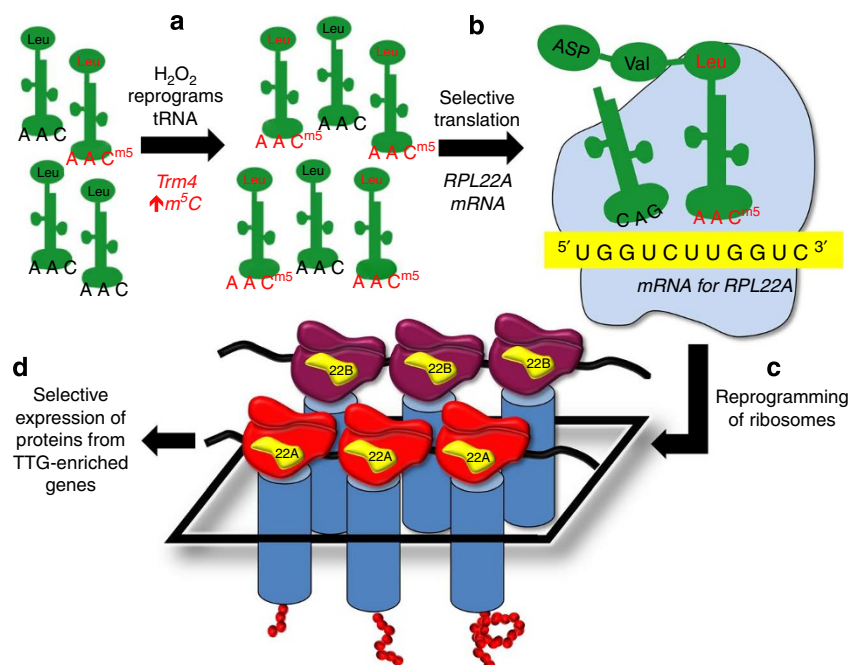


Figure 7 | Proposed mechanism by which increase in m⁵C level regulates translation of ribosomal protein paralogues and confers resistance to H₂O₂. Exposure to H₂O₂ leads to an elevation in the level of m⁵C at the wobble position of the leucine tRNA for translating the codon UUG on mRNA (a), which enhances the translation of the UUG-enriched RPL22A mRNA relative to its paralogue RPL22B (b) and leads to changes in ribosome composition (c). This reprogramming of tRNA and ribosomes ultimately causes selective translation of proteins from genes enriched with the codon TTT (d).

collected by centrifugation (1,500g, 10 min, 4 °C), and washed twice with ice-cold H₂O. Cells were lysed by suspension in 2 M NaOH, 8% 2-mercaptoethanol (v/v). Following TCA precipitation, proteins were pelleted by centrifugation (15,000g, 15 min, 4 °C) and the pellet was resuspended in 8 M urea, 75 mM NaCl, 50 mM Tris, pH 8.2, 50 mM NaF, 50 mM β-glycerophosphate, 1 mM sodium orthovanadate, 10 mM sodium pyrophosphate and 1 mM phenylmethylsulphonyl fluoride⁴⁴. Protein concentration was determined by the Bradford assay⁴⁵. Heavy SILAC-labeled *lys1Δ* yeast proteins were used as a global internal standard³⁰. Following addition of internal standard to all treated and untreated wild-type and *trm4Δ* yeast protein samples (1:1), the protein mixture was reduced in 1 M dithiothreitol (2.5 h, 37 °C), alkylated with iodoacetamide (5.5 mM, 40 min, ambient temperature, dark) and then digested with 50:1 (w/w) trypsin (14 h, 37 °C).

Peptide mixtures were loaded onto a Vydac C18 trap column (150 μm × 10 mm, 5 μm, 300 Å particle; Grace, Deerfield, IL) at 5 μl min⁻¹ and eluted onto a Vydac C18 analytical column (75 μm × 150 mm, 5 μm per 300 Å particle) at 200 nl min⁻¹ with a 120 min gradient of 2–98% acetonitrile in 0.1% formic acid. Eluted peptides were analysed by MS analysis on a QSTAR-XL (Applied Biosystems, Foster City, CA). Acquired MS/MS spectra were parsed by Spectrum Mill and searched against Swiss-Prot database. CID spectra of tryptic peptides were searched against the database sequences within a mass window of 100 p.p.m. for precursor ion searches and 500 p.p.m. for fragment ions. Database search results were filtered based on Spectrum Mill scoring criteria, which include peptide score, a measure of confidence of identification, and scored peak intensity (SPI) that represents the percentage of assigned peaks in CID spectrum. Peptide search results with a score ≥ 6, SPI ≥ 60% and no missed cleavages were used for protein quantification. SILAC peptide and protein quantification was performed with differential expression quantification and SILAC protein ratios were determined as the average of all peptide ratios assigned to the protein. Differential protein expression was determined by Student's *t*-test for four biological replicates. A summary of identified proteins and their expression levels are presented in Supplementary Data 1. The proteomics data has been deposited in the PeptideAtlas database (www.peptideatlas.org) under the accession code PASS00059.

Gene ontology annotation. Gene functional categorization and pathway analysis were performed with DAVID Bioinformatics Resources 2011 (ref. 46). The annotated proteins are clustered according to the biological process branch of the GO annotation. The statistical significance of over-representation or under-representation of proteins in each GO category was assessed using a hypergeometric distribution and the significance indicated by the *P* values for each GO category.

References

1. Rozenski, J., Crain, P. F. & McCloskey, J. A. The RNA modification database: 1999 update. *Nucleic Acids Res.* **27**, 196–197 (1999).

2. Czerwoniec, A. *et al.* MODOMICS: a database of RNA modification pathways. 2008 update. *Nucleic Acids Res.* **37**, D118–D121 (2009).
3. Söll, D. & RajBhandary, U. *tRNA: Structure, Biosynthesis and Function* (ASM Press, 1995).
4. Limbach, P. A., Crain, P. F. & McCloskey, J. A. Summary: the modified nucleosides of RNA. *Nucleic Acids Res.* **22**, 2183–2196 (1994).
5. Agris, P. F., Vendeix, F. A. & Graham, W. D. tRNA's wobble decoding of the genome: 40 years of modification. *J. Mol. Biol.* **366**, 1–13 (2007).
6. Yarian, C. *et al.* Accurate translation of the genetic code depends on tRNA modified nucleosides. *J. Biol. Chem.* **277**, 16391–16395 (2002).
7. Urbonavicius, J., Qian, Q., Durand, J. M., Hagervall, T. G. & Bjork, G. R. Improvement of reading frame maintenance is a common function for several tRNA modifications. *EMBO J.* **20**, 4863–4873 (2001).
8. Bjork, G. R. *et al.* Transfer RNA modification: influence on translational frameshifting and metabolism. *FEBS Lett.* **452**, 47–51 (1999).
9. Motorin, Y. & Helm, M. tRNA stabilization by modified nucleotides. *Biochemistry* **49**, 4934–4944 (2010).
10. Alexandrov, A. *et al.* Rapid tRNA decay can result from lack of nonessential modifications. *Mol. Cell* **21**, 87–96 (2006).
11. Thompson, D. M. & Parker, R. Stressing out over tRNA cleavage. *Cell* **138**, 215–219 (2009).
12. Begley, U. *et al.* Trm9-catalyzed tRNA modifications link translation to the DNA damage response. *Mol. Cell* **28**, 860–870 (2007).
13. Netzer, N. *et al.* Innate immune and chemically triggered oxidative stress modifies translational fidelity. *Nature* **462**, 522–526 (2009).
14. Emilsson, V., Naslund, A. K. & Kurland, C. G. Thiolation of transfer RNA in *Escherichia coli* varies with growth rate. *Nucleic Acids Res.* **20**, 4499–4505 (1992).
15. Begley, T. J., Rosenbach, A. S., Ideker, T. & Samson, L. D. Hot spots for modulating toxicity identified by genomic phenotyping and localization mapping. *Mol. Cell* **16**, 117–125 (2004).
16. Bennett, C. B. *et al.* Genes required for ionizing radiation resistance in yeast. *Nat. Genet.* **29**, 426–434 (2001).
17. Rooney, J. P. *et al.* Systems based mapping demonstrates that recovery from alkylation damage requires DNA repair, RNA processing, and translation associated networks. *Genomics* **10**, 524 (2008).
18. Kalhor, H. R. & Clarke, S. Novel methyltransferase for modified uridine residues at the wobble position of tRNA. *Mol. Cell Biol.* **23**, 9283–9292 (2003).
19. Weissbach, J. & Dirheimer, G. Pairing properties of the methylester of 5-carboxymethyl uridine in the wobble position of yeast tRNA³Arg. *Biochim. Biophys. Acta.* **518**, 530–534 (1978).

20. Chan, C. T. *et al.* A quantitative systems approach reveals dynamic control of tRNA modifications during cellular stress. *PLoS Genet.* **6**, e1001247 (2010).
21. Strobel, M. C. & Abelson, J. Effect of intron mutations on processing and function of *Saccharomyces cerevisiae* SUP53 tRNA *in vitro* and *in vivo*. *Mol. Cell Biol.* **6**, 2663–2673 (1986).
22. Plant, E. P. *et al.* Differentiating between near- and non-cognate codons in *Saccharomyces cerevisiae*. *PLoS One* **2**, e517 (2007).
23. Tumu, S., Patil, A., Towns, W., Dyavaiah, M. & Begley, T. J. The Gene Specific Codon Usage Database: a genome-based catalog of one, two, three, four and five codon combinations present in *Saccharomyces cerevisiae* genes. *Database* **2012**, bas002 (2012).
24. Kellis, M., Birren, B. W. & Lander, E. S. Proof and evolutionary analysis of ancient genome duplication in the yeast *Saccharomyces cerevisiae*. *Nature* **428**, 617–624 (2004).
25. Baudin-Baillieu, A., Tollervey, D., Cullin, C. & Lacroute, F. Functional analysis of Rrp7p, an essential yeast protein involved in pre-rRNA processing and ribosome assembly. *Mol. Cell Biol.* **17**, 5023–5032 (1997).
26. Enyenihi, A. H. & Saunders, W. S. Large-scale functional genomic analysis of sporulation and meiosis in *Saccharomyces cerevisiae*. *Genetics* **163**, 47–54 (2003).
27. Haarer, B., Viggiano, S., Hibbs, M. A., Troyanskaya, O. G. & Amberg, D. C. Modeling complex genetic interactions in a simple eukaryotic genome: actin displays a rich spectrum of complex haploinsufficiencies. *Genes Dev.* **21**, 148–159 (2007).
28. Ni, L. & Snyder, M. A genomic study of the bipolar bud site selection pattern in *Saccharomyces cerevisiae*. *Mol. Biol. Cell* **12**, 2147–2170 (2001).
29. Komili, S., Farny, N. G., Roth, F. P. & Silver, P. A. Functional specificity among ribosomal proteins regulates gene expression. *Cell* **131**, 557–571 (2007).
30. Ishihama, Y. *et al.* Quantitative mouse brain proteomics using culture-derived isotope tags as internal standards. *Nat. Biotechnol.* **23**, 617–621 (2005).
31. Mauro, V. P. & Edelman, G. M. The ribosome filter redux. *Cell Cycle* **6**, 2246–2251 (2007).
32. Liu, D. & Xu, Y. p53, oxidative stress, and aging. *Antioxid. Redox. Signal* **15**, 1669–1678 (2011).
33. Takagi, M., Absalon, M. J., McLure, K. G. & Kastan, M. B. Regulation of p53 translation and induction after DNA damage by ribosomal protein L26 and nucleolin. *Cell* **123**, 49–63 (2005).
34. Nakao, A., Yoshihama, M. & Kenmochi, N. RPG: the ribosomal protein gene database. *Nucleic Acids Res.* **32**, D168–D170 (2004).
35. Holcik, M. & Sonenberg, N. Translational control in stress and apoptosis. *Nat. Rev. Mol. Cell Biol.* **6**, 318–327 (2005).
36. Wood, J., Frederickson, R. M., Fields, S. & Patel, A. H. Hepatitis C virus 3'X region interacts with human ribosomal proteins. *J. Virol.* **75**, 1348–1358 (2001).
37. Anderson, S. J. *et al.* Ablation of ribosomal protein L22 selectively impairs alphabeta T cell development by activation of a p53-dependent checkpoint. *Immunity* **26**, 759–772 (2007).
38. Dobbstein, M. & Shenk, T. *In vitro* selection of RNA ligands for the ribosomal L22 protein associated with Epstein-Barr virus-expressed RNA by using randomized and cDNA-derived RNA libraries. *J. Virol.* **69**, 8027–8034 (1995).
39. Le, S., Sternglanz, R. & Greider, C. W. Identification of two RNA-binding proteins associated with human telomerase RNA. *Mol. Biol. Cell* **11**, 999–1010 (2000).
40. Toczyski, D. P. & Steitz, J. A. EAP, a highly conserved cellular protein associated with Epstein-Barr virus small RNAs (EBERs). *EMBO J.* **10**, 459–466 (1991).
41. Dlakic, M. The ribosomal subunit assembly line. *Genome Biol.* **6**, 234 (2005).
42. Yewdell, J. W. & Nicchitta, C. V. The DRIP hypothesis decennial: support, controversy, refinement and extension. *Trends Immunol.* **27**, 368–373 (2006).
43. de Godoy, L. M. *et al.* Comprehensive mass-spectrometry-based proteome quantification of haploid versus diploid yeast. *Nature* **455**, 1251–1254 (2008).
44. Gruhler, A. *et al.* Quantitative phosphoproteomics applied to the yeast pheromone signaling pathway. *Mol. Cell Proteomics* **4**, 310–327 (2005).
45. Bradford, M. M. A rapid and sensitive method for the quantitation of microgram quantities of protein utilizing the principle of protein-dye binding. *Anal. Biochem.* **72**, 248–254 (1976).
46. Huang da, W., Sherman, B. T. & Lempicki, R. A. Systematic and integrative analysis of large gene lists using DAVID bioinformatics resources. *Nat. Protoc.* **4**, 44–57 (2009).

Acknowledgements

We thank Professor Wendy Gilbert (Department of Biology, MIT) for assistance with ribosome purification. We also thank Drs. Koli Taghizadeh and John Wishnok for assistance with mass spectrometry, which was performed in the Bioanalytical Facilities Core of the MIT Center for Environmental Health Sciences. Financial support was provided by the National Institute of Environmental Health Sciences (ES002109, ES017010, ES015037 and ES017010), the MIT Westaway Fund, a Merck–MIT Graduate Student Fellowship (C.T.Y.C.) and the Singapore-MIT Alliance for Research and Technology.

Author contributions

All authors contributed to experimental design, data analysis and interpretation, and preparation of the manuscript. C.T.Y.C., Y.L.J.P., W.D. and M.D. contributed to performance of the experiments.

Additional information

Accession codes: The proteomics data have been deposited in the PeptideAtlas database (www.peptideatlas.org) under the accession code PASS00059.

Supplementary Information accompanies this paper at <http://www.nature.com/naturecommunications>

Competing financial interests: The authors declare no competing financial interests.

Reprints and permission information is available online at <http://npg.nature.com/reprintsandpermissions/>

How to cite this article: Chan, C.T.Y. *et al.* Reprogramming of tRNA modifications controls the oxidative stress response by codon-biased translation of proteins. *Nat. Commun.* **3**:937 doi: 10.1038/ncomms1938 (2012).